GEOPHYSICAL RESEARCH LETTERS, VOL. 34, L19505, doi:10.1029/2007GL031480, 2007

Increasing solar heating of the Arctic Ocean and adjacent seas, 1979–2005: Attribution and role in the ice-albedo feedback

Donald K. Perovich,[1] Bonnie Light,[2] Hajo Eicken,[3] Kathleen F. Jones,[1] Kay Runciman,[2] and Son V. Nghiem[4]

Received 26 July 2007; revised 30 August 2007; accepted 12 September 2007; published 11 October 2007.

[1] Over the past few decades the Arctic sea ice cover has decreased in areal extent. This has altered the solar radiation forcing on the Arctic atmosphere-ice-ocean system by decreasing the surface albedo and allowing more solar heating of the upper ocean. This study addresses how the amount of solar energy absorbed in areas of open water in the Arctic Basin has varied spatially and temporally over the past few decades. A synthetic approach was taken, combining satellite-derived ice concentrations, incident irradiances determined from reanalysis products, and field observations of ocean albedo over the Arctic Ocean and the adjacent seas. Results indicate an increase in the solar energy deposited in the upper ocean over the past few decades in 89% of the region studied. The largest increases in total yearly solar heat input, as much as 4% per year, occurred in the Chukchi Sea and adjacent areas.
Citation: Perovich, D. K., B. Light, H. Eicken, K. F. Jones, K. Runciman, and S. V. Nghiem (2007), Increasing solar heating of the Arctic Ocean and adjacent seas, 1979–2005: Attribution and role in the ice-albedo feedback, *Geophys. Res. Lett.*, *34*, L19505, doi:10.1029/2007GL031480.

1. Introduction

[2] The importance of the Arctic sea-ice cover in the global climate system is largely derived from its central role in driving northern hemisphere ice-albedo feedback [*Holland and Bitz*, 2003; *Hall*, 2004]. This feedback results from the large contrast between the albedos of sea ice (>0.6) and open water (~0.07). General circulation models (GCMs) consistently show that a reduction in sea-ice area driven by changes in external forcing (such as increasing greenhouse gas concentrations) is substantially enhanced through resulting increases in solar heat input into open water [*Holland and Bitz*, 2003; *Zhang and Walsh*, 2006]. While GCMs indicate that such ice-albedo feedback plays an important role in polar amplification of climate change, few studies have examined this process in detail [*Robock*, 1983; *Hall*, 2004]. Observational records indicate that the Arctic perennial ice cover has been shrinking substantially over the past few decades [*Stroeve et al.*, 2005; *Serreze et al.*, 2007a]. Recent work furthermore suggests that the reduction in ice extent is at rates higher than predicted by the models employed in the Intergovernmental Panel on Climate Change Fourth Assessment Report [*Stroeve et al.*, 2007]. These reductions in sea ice have been related to changes in longwave radiative fluxes, atmospheric circulation and ocean heat flux [e.g., *Rigor et al.*, 2002; *Rigor and Wallace*, 2004; *Lindsay and Zhang*, 2005; *Francis and Hunter*, 2006].

[3] In this paper we examine the role of solar heating of the open water in the ice pack and explore trends in heat input by determining the amount of solar heating of open water, both within the perennial ice pack as well as the seasonally ice-free ocean, over the entire maximum extent of the Arctic sea-ice zone. This analysis extends from 1979 to 2005 and synthesizes solar irradiances derived as daily mean values from a numerical weather reanalysis, ice concentrations determined from passive microwave satellite data, and measurements of the ocean albedo during summer. We present maps of the input of solar shortwave energy into the ocean and discuss solar heating trends observed over the past two decades in the context of observed changes in the ice cover and ice-albedo feedback.

2. Methods

[4] The flux of solar heat input directly to the ocean (F_{rw}) depends on the incident solar irradiance (F_r), the ice concentration (C), and the albedo of the ocean (α) and can be expressed as

$$F_{rw} = F_r(1-\alpha)(1-C). \quad (1)$$

In this analysis, we consider only the solar energy incident on the open ocean. No attempt was made to estimate the penetration of radiation through the ice cover. As a result, this approach represents a lower bound on the total solar heating of the upper ocean. To evaluate equation 1 every day at every grid cell, F_r, C and α must be known as a function of time and location. *Pegau and Paulson* [2001] determined that while the albedo of open water in Arctic pack ice had modest variations due to solar zenith angle and cloud conditions, a value of 0.07 was typical and representative. The ocean albedo is set equal to 0.07 for all calculations in this paper.

[5] Values of F_r are determined from ERA-40 reanalysis (1979–2001) and from operational European Center for Medium-Range Weather Forecasts products (2002–2005). The ERA-40 reanalysis has demonstrated considerable skill

[1]Cold Regions Research and Engineering Laboratory, U.S. Army Engineer Research and Development Center, Hanover, New Hampshire, USA.
[2]Polar Science Center, Applied Physics Laboratory, Seattle, Washington, USA.
[3]Geophysical Institute, University of Alaska Fairbanks, Fairbanks, Alaska, USA.
[4]Jet Propulsion Laboratory, California Institute of Technology, Pasadena, California, USA.

0094-8276/07/2007GL031480$05.00

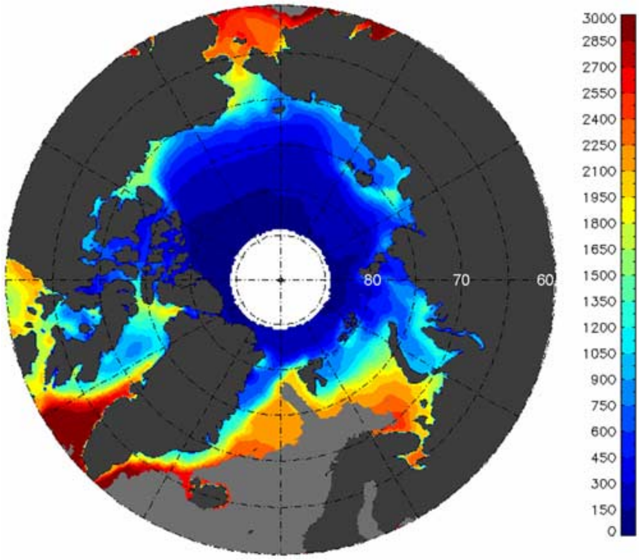

Figure 1. Map of mean total annual solar input averaged over 1979–2005 (units are in MJ m^{-2}).

in the Arctic [*Liu et al.*, 2005; *Serreze et al.*, 2007b]. In particular, *Liu et al.* [2005] demonstrate that the ERA-40 downwelling shortwave flux data show good agreement with observation and negligible long-term bias. No large discontinuities were evident between the ERA-40 and ECMWF incident irradiance. Limited studies [*Xie et al.*, 2006] have indicated good accuracy in ECMWF incident solar irradiance data. Data are mapped onto a 25 km × 25 km Equal Area Scalable Earth (EASE) grid. The region of interest is the area north of 60° latitude where ice is present some time during the period of investigation (contoured area in Figure 1).

[6] Ice concentrations are determined from remotely sensed passive microwave observations using the NASA Team Algorithm [*Cavalieri et al.*, 1990] (accessed in 2007). Accurate determination of the ice concentration during the summer melt season from passive microwave sensors is recognized as a problem due to difficulties in differentiating between open water and melt ponds. Differences in several passive microwave algorithms have been estimated and compared with ice charts independently derived from RADARSAT synthetic aperture radar, Operational Linescan System, and Advanced Very High Resolution Radiometer data [*Partington*, 2000]. The NASA Team Algorithm (NT) has been improved [*Markus and Cavalieri*, 2000] and tested [*Markus and Dokken*, 2002] in response to these difficulties. Applying this NASA Team 2 (NT2) algorithm, the latter study found biases to be negligible in the Central Arctic and about −5% in the marginal ice zone. We compared three different ice concentration data sets, derived from NT and NT2, as well as a merged data set based on NT and other sources of data, including a bias correction, compiled as part of the ERA-40 reanalysis efforts [*Fiorino*, 2004]. Comparing these different data sets and resulting data on solar heating of water within the ice pack for one entire year (1998), and taking into consideration that NT2 data are least impacted by the presence of surface meltwater on the ice [*Markus and Dokken*, 2002], we find that both ERA-40 and NT ice concentrations exhibit a positive bias in amount of solar heating ranging mostly between 20 and 40% of the total annual input relative to NT2. The ERA-40 data set exhibits much less spatial variability in ice concentration than the satellite results. Hence, we chose to work with the NT data set and recognize that the total annual solar heating exhibits a bias as outlined above. However, this systematic error due to underestimation of summer ice concentrations should not impact year-to-year trends in solar heat input. Furthermore, as shown in detail below, the regions exhibiting highly significant trends fall into areas in the lower bias range (estimated at around 20%).

[7] Equation 1 is evaluated at every grid cell each day from 1979 through 2005. Missing data are estimated using linear interpolation in time. The daily input of solar heat to the ocean (q_w) is computed by multiplying F_{rw} calculated in equation 1 by the number of seconds in a day. Annual cumulative amounts of solar heat (Q_w) are tabulated by summing the daily values for each year. Mean values of Q_w were subtracted from each annual value to produce annual anomalies.

[8] Best-fit straight lines for the anomalies at each grid point are used to determine the time-dependent linear trend in the cumulative solar heat input in MJ m^{-2} yr^{-1}. The fraction of the variance explained by the linear least squares fit (R^2) is computed. Trends in heat input are also divided by the mean at each grid point and multiplied by 100 to give percent change in solar heat input per year.

3. Results

[9] The mean annual cumulative heat input averaged over the period 1979–2005 is plotted in Figure 1. Values range from a few hundred MJ m^{-2} at high latitudes in the perennial ice regime to a few thousand MJ m^{-2} at lower latitudes in the seasonal ice zone. The patterns in solar heat input to the ocean reflect the latitudinal dependence of incident irradiance – apparent in the data's radial symmetry and decreasing trend towards the Pole, in conjunction with regional variations in ice concentration and ice motion. The latter is evident in the distortion of radial symmetry from eastern longitudes towards the Canadian Archipelago, where ice concentrations tend to be larger due to ice circulation patterns. The largest values of solar input occur in the seasonal ice zone, particularly in the Bering Sea, Davis Strait, and Greenland Sea, where ice retreat typically begins in late spring or early summer. There are also strong longitudinal variations at lower latitudes particularly in the Davis Strait region and between the Barents and Kara seas.

[10] The trends in solar heat input directly to the ocean for each grid cell from 1979 to 2005 are mapped in Figure 2. Positive trends are pervasive over much of the Arctic with values as large as 4% per year in two areas centered at 75°N, 165°W, in the Chukchi Sea and at 75°N, 80°E in the Kara Sea. A smaller spatially coherent elongated region with a negative trend in solar heat input is evident along the northern edge of the Canadian Archipelago, where ice motion has caused increases in ice concentration.

[11] Of the 24,744 grid cells, 89% have a positive trend and 11% a negative trend. Trends were typically modest in magnitude, with 40% of all grid cells lying between −0.5% and +0.5% yr^{-1}.The median and mean of the trends were an

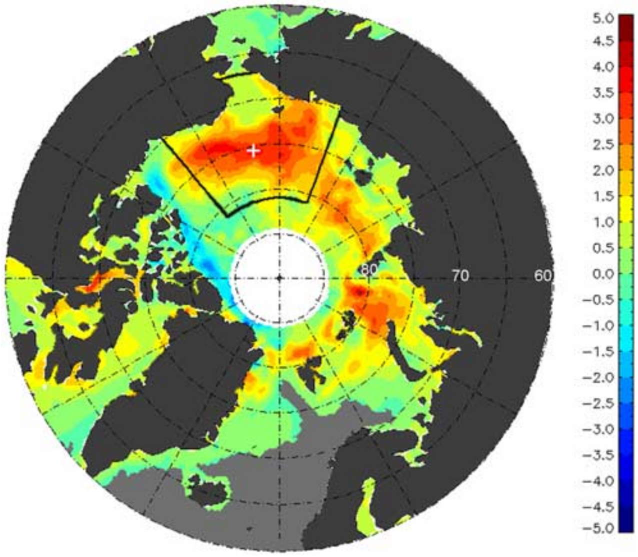

Figure 2. Map of the linear trend of annual solar heat input to the ocean, with units of percent per year. The subregion of interest is defined by the black border. The white plus sign denotes the area presented in Figure 3.

increase of 0.64% yr^{-1} and 0.81% yr^{-1} respectively. Due to the large interannual variability in heat input and the small trends, most values of fraction of the variance explained by the linear least squares fits (R^2) are less than 0.2. The largest values of R^2 (0.6 to 0.8) are co-located with the largest warming trend in the northern Chukchi Sea and adjacent Arctic Ocean.

4. Discussion

[12] From 1979 through 2005 there was a pervasive increase in the amount of solar energy deposited in the upper Arctic Ocean and surrounding seas, with maximum values of 4% per year, despite considerable interannual and spatial variability. As equation 1 indicates, the solar heat input to the ocean is a function of the ice concentration and the incident solar irradiance. To explore the relative importance of changes in ice concentration and incident irradiance, we calculated trends in these two parameters from 1979 to 2005. For 65% of the grid cells there was a trend of decreasing solar incident irradiance, which would decrease the solar heat input to the ocean. In contrast, 85% of the grid cells showed a decreasing trend in ice concentration, resulting in more heat input to the ocean.

[13] These results indicate that the decrease in ice concentration (e.g. increase in open water fraction) is primarily responsible for the trend of increasing solar heat input to the ocean. To further examine this finding, we computed the linear correlation coefficient of the annual solar heat to the ocean with the average annual open water fraction ($1 - C$) and with the annual total incident solar irradiance at each grid point using the 27-yr record. There is a predominantly positive correlation between solar heat input and open water fraction over much of the area, with correlations between 0.7 and 1.0 for 75% of the grid cells. The correlation is strongest (0.9 to 1.0), where the trend of increasing solar heat input is greatest. Correlations greater than about 0.5 are significant at the 1% level; that is, the probability that these values are drawn from populations that are actually uncorrelated is less than 1%.

[14] The correlation between solar heat input and the incident solar irradiance was weak over most of area, with half of the grid cells having values between −0.2 and 0.2 suggesting that changes in incident irradiance have not driven the observed trends in solar heat input to the ocean. There were strong correlations in the marginal ice zone near Greenland, which is ice free for much of the summer and variations in incident solar irradiance dominate the solar heat input. Overall the trend of increasing solar heat input to the ocean was correlated with a trend of decreasing ice concentration.

[15] While the annual trends in solar heat input may be modest, the cumulative effect is significant. Transforming the trends from percent to energy results in a median of 5.7 MJ m^{-2} yr^{-1} and a mean of 6.6 MJ m^{-2} yr^{-1}. The mean and median trends appear rather small; a few cm per year of ice thinning, less than one W m^{-2} of additional heat flux per year. But these trends in heat input are cumulative and after a few decades the total changes are substantial. For example, the median increase of 0.64% yr^{-1} accumulates to a total increase of 17% by 2005. Integrating over the entire study region from 1979 to 2005, the total additional heat input is 2.9×10^{15} MJ. This is enough heat to melt 9.3×10^{12} m^3 of ice.

[16] The time series of annual solar heat input is examined in more detail in Figure 3 for the region where the increasing trend has been strongest (75 × 50 km area centered on 76°N, 170°W). Plotted are the percent anomalies in annual incident irradiance, open water fraction, and solar heat input. A strong relationship (correlation = 0.94) between solar heat input and open water fraction is evident in how closely the curves track in the plot. Changes in incident irradiance are smaller and not correlated with solar heat input (correlation = −0.35). A general increasing trend in solar heat input is evident, with interannual variability

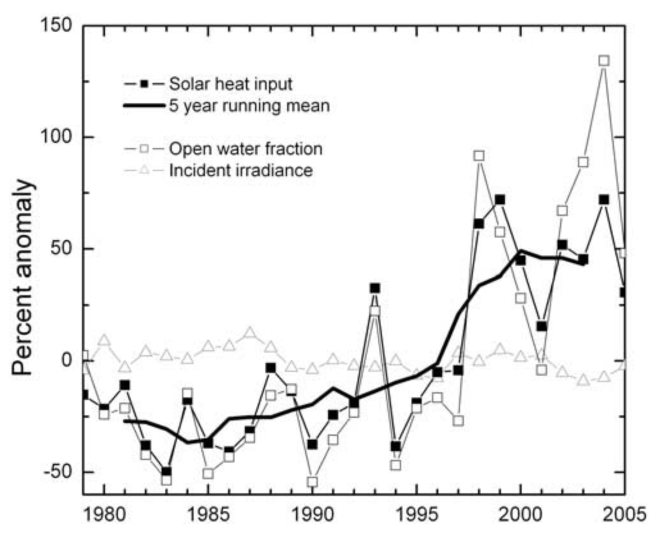

Figure 3. Time series of anomaly in annual solar heat input, open water fraction, and incident irradiance for a 75 km × 50 km area centered on 76°N, 170°W. The thick line is the five year running mean of solar heat input.

exceeding a factor of two. A five-year running mean eliminates these fluctuations and reveals that solar heat input was fairly constant from 1979 to 1992 and then steadily increased through 2005. The overall increase was from an annual value of approximately 200 MJ m^{-2} to about 400 MJ m^{-2}. A key question is whether this increase is accelerating or staying constant. Unfortunately the time series is too short to determine whether this increase is linear or non-linear in nature (linear, quadratic, logarithmic, exponential, or power-law least-squares models all yield correlation coefficients greater than 0.95).

[17] Incremental solar heating of a specific area can lead to progressive thinning of ice, eventually expressed in reduced ice concentrations. At the same time, other factors have been shown to contribute to ice retreat in the region north of Alaska, such as changes in surface circulation and less extensive multiyear ice [*Tucker et al.*, 2001; *Perovich et al.*, 2003; *Shimada et al.*, 2006]. The role of the upper ocean in driving or sustaining part of the reduction in summer ice cover is not clear [*Serreze et al.*, 2007a]. *Woodgate et al.* [2006] found both substantial interannual variability (1990–2004) as well as a significant increase in heat transport through Bering Strait in the early 2000s. Such an increase may play a role in further amplifying ice retreat in the adjacent sectors of the Chukchi Sea. However, in magnitude the advected heat flux accounts for at most between one fifth and one half of the increase in solar heat input examined here. Thus, the sub-region defined in Figure 2 experienced solar heat input of 14.6×10^{14} MJ in 2005, compared to 9.2×10^{14} MJ in 1979. It is unclear whether increased advection of heat in the Atlantic water layer of the Arctic Ocean [*Polyakov et al.*, 2005] has contributed to ice thinning, as this water mass resides well below the Arctic halocline and the Bering inflow [*Woodgate et al.*, 2006].

[18] An important question is how increased solar heating during the summer months impacts ice growth and melt in the subsequent year. *Shimada et al.* [2006] invoke changes in the wind-driven ice circulation as an important mechanism of preserving ice-extent anomalies. *Francis and Hunter*'s [2006] study suggests that at least in the 1990s and early 2000s, increased downward longwave fluxes (promoted by reduced ice concentration) may be one way for ice extent anomalies to persist. However, equally effective would be a capping of the upper ocean by sea ice before much of the solar heat has been extracted in late fall, retaining the warming signal within the ocean-ice system throughout winter and spring. Evidence of substantial winter ice-bottom melt and halocline warming throughout the Chukchi Sea [*Perovich et al.*, 2003; *Shimada et al.*, 2006] suggest that this process is important, though its full extent and the processes fostering such longer-term preservation of warming signals are not well understood.

[19] *Francis and Hunter* [2006] found that roughly 40% of the variance in summer-minimum ice extent anomalies in the Chukchi Sea (1979–2004) is explained by atmospheric forcing (primarily downward longwave radiative fluxes). Our work raises the question whether changes in surface regional albedo due to changing ice concentrations and earlier ice retreat may explain a significant fraction of the remainder of the ice-extent anomaly variance. While quantitative attribution requires further work, the coherent spatial patterns of ice retreat and increases in solar heating shown in Figure 2 nevertheless suggest that ice-albedo feedback plays an important role in explaining the observed ice thinning and reduction in ice extent in the northern Chukchi Sea and adjacent Arctic Ocean.

[20] Solar energy deposited in the ocean may cause melting on the lateral edges or on the bottom of ice floes. However, not all of the additional absorbed solar heat will contribute to ice melting. Some heat will also be lost to the atmosphere or stored in the ocean. The partitioning of the additional solar heat input to the ocean will strongly influence the magnitude of the ice-albedo feedback and the overall heat and mass budget of the ice cover. For example, enhanced lateral melting will directly impact the ice-albedo feedback by reducing the ice concentration and further increasing the solar heat input to the ocean. In contrast, energy stored in the ocean will retard freezing in the fall, but may not contribute significantly to the ice-albedo feedback.

[21] Understanding the interaction of solar energy with the ice cover and determining how much solar energy is reflected by or absorbed in the ice, or transmitted to the ocean is more complex than the ocean partitioning. This is primarily because of the seasonal evolution of ice albedo, which depends on the characteristics of the snow cover in spring and melt ponds in summer [*Perovich et al.*, 2002; *Perovich et al.*, 2007]. Although limited to open water areas, the present findings clearly demonstrate the importance of ice-albedo feedback in explaining drastic reductions in ice extent in the Western Arctic and overall represent a lower limit on the amount of additional heat provided to the ocean in the wake of a thinning and shrinking ice cover.

[22] **Acknowledgments.** Thanks to Axel Schweiger for providing the ECMWF data for 2002–2005. This work has been funded by the Arctic System Science program at the National Science Foundation as part of the Synthesis of Arctic System Science under contract numbers ARC-0531026 and ARC-0531018. The research carried out at the Jet Propulsion Laboratory, California Institute of Technology, was supported under a contract with the National Aeronautics and Space Administration Cryospheric Sciences Program.

References

Cavalieri, D., P. Gloersen, and J. Zwally (1990), DMSP SSM/I daily polar gridded sea ice concentrations, edited by J. Maslanik and J. Stroeve, http://nsidc.org/data/docs/daac/nsidc0002_ssmi_seaice.gd.html, Natl. Snow and Ice Data Cent. (NSDIC) DAAC, Boulder, Colo.

Fiorino, M. (2004), A multi-decadal daily sea surface temperature and sea ice concentration data set for the ERA-40 reanalysis, *ERA-40 Proj. Rep. Ser. 12*, pp. 1–22, Eur. Cent. for Medium Range Weather Forecasts, Reading, U. K.

Francis, J. A., and E. Hunter (2006), New insight into the disappearing Arctic sea ice, *Eos Trans. AGU*, *87*(46), 509.

Hall, A. (2004), The role of surface albedo feedback in climate, *J. Clim.*, *17*, 1550–1568.

Holland, M. M., and C. M. Bitz (2003), Polar amplification of climate change in coupled models, *Clim. Dyn.*, *21*, 221–232.

Lindsay, R. W., and J. Zhang (2005), The thinning of Arctic sea ice, 1988–2003: Have we passed a tipping point?, *J. Clim.*, *18*, 4879–4894.

Liu, J., J. A. Curry, W. B. Rossow, J. R. Key, and X. Wang (2005), Comparison of surface radiative flux data sets over the Arctic Ocean, *J. Geophys. Res.*, *110*, C02015, doi:10.1029/2004JC002381.

Markus, T., and D. J. Cavalieri (2000), An enhancement of the NASA Team sea ice algorithm, *IEEE Trans. Geosci. Remote Sens.*, *38*(3), 1387–1398.

Markus, T., and S. T. Dokken (2002), Evaluation of Arctic late summer passive microwave sea ice retrievals, *IEEE Trans. Geosci. Remote Sens.*, *40*(2), 348–356.

Partington, K. C. (2000), A data fusion algorithm for mapping sea-ice concentrations from Special Sensor Microwave/Imager data, *IEEE Trans. Geosci. Remote Sens.*, *38*(4), 1947–1958.

Pegau, W. S., and C. A. Paulson (2001), The albedo of Arctic leads in summer, *Ann. Glaciol.*, *33*, 221–224.
Perovich, D. K., T. C. Grenfell, B. Light, and P. V. Hobbs (2002), Seasonal evolution of the albedo of multiyear Arctic sea ice, *J. Geophys. Res.*, *107*(C10), 8044, doi:10.1029/2000JC000438.
Perovich, D. K., T. C. Grenfell, J. A. Richter-Menge, B. Light, W. B. Tucker III, and H. Eicken (2003), Thin and thinner: Sea ice mass balance measurements during SHEBA, *J. Geophys. Res.*, *108*(C3), 8050, doi:10.1029/2001JC001079.
Perovich, D. K., S. V. Nghiem, T. Markus, and A. Schweiger (2007), Seasonal evolution and interannual variability of the local solar energy absorbed by the Arctic sea ice–ocean system, *J. Geophys. Res.*, *112*, C03005, doi:10.1029/2006JC003558.
Polyakov, I. V., et al. (2005), One more step toward a warmer Arctic, *Geophys. Res. Lett.*, *32*, L17605, doi:10.1029/2005GL023740.
Rigor, I., and J. M. Wallace (2004), Variations in the age of Arctic sea-ice and summer sea-ice extent, *Geophys. Res. Lett.*, *31*, L09401, doi:10.1029/2004GL019492.
Rigor, I. G., J. M. Wallace, and R. L. Colony (2002), Response of sea ice to the Arctic Oscillation, *J. Clim.*, *15*, 2648–2663.
Robock, A. (1983), Ice and snow feedbacks and the latitudinal and seasonal distribution of climate sensitivity, *J. Atmos. Sci.*, *40*, 986–997.
Serreze, M. C., M. M. Holland, and J. Stroeve (2007a), Perspectives on the Arctic's shrinking sea ice cover, *Science*, *315*, 1533–1536.
Serreze, M. C., A. P. Barrett, A. G. Slater, M. Steele, J. Zhang, and K. E. Trenberth (2007b), The large-scale energy budget of the Arctic, *J. Geophys. Res.*, *112*, D11122, doi:10.1029/2006JD008230.
Shimada, K., T. Kamoshida, M. Itoh, S. Nishino, E. Carmack, F. McLaughlin, S. Zimmermann, and A. Proshutinsky (2006), Pacific Ocean inflow: Influence on catastrophic reduction of sea ice cover in the Arctic Ocean, *Geophys. Res. Lett.*, *33*, L08605, doi:10.1029/2005GL025624.
Stroeve, J., M. C. Serreze, F. Fetterer, T. Arbetter, W. Meier, J. Maslanik, and K. Knowles (2005), Tracking the Arctic's shrinking ice cover: Another extreme September minimum in 2004, *Geophys. Res. Lett.*, *32*, L04501, doi:10.1029/2004GL021810.
Stroeve, J., M. M. Holland, W. Meier, T. Scambos, and M. Serreze (2007), Arctic sea ice decline: Faster than forecast, *Geophys. Res. Lett.*, *34*, L09501, doi:10.1029/2007GL029703.
Tucker, W. B. I., J. W. Weatherly, D. T. Eppler, D. Farmer, and D. L. Bentley (2001), Evidence for the rapid thinning of sea ice in the western Arctic Ocean at the end of the 1980s, *Geophys. Res. Lett.*, *28*, 2851–2854.
Woodgate, R. A., K. Aagaard, and T. J. Weingartner (2006), Interannual changes in the Bering Strait fluxes of volume, heat and freshwater between 1991 and 2004, *Geophys. Res. Lett.*, *33*, L15609, doi:10.1029/2006GL026931.
Xie, S., S. A. Klein, J. J. Yio, A. C. M. Beljaars, C. N. Long, and M. Zhang (2006), An assessment of ECMWF analyses and model forecasts over the North Slope of Alaska using observations from the ARM Mixed-Phase Arctic Cloud Experiment, *J. Geophys. Res.*, *111*, D05107, doi:10.1029/2005JD006509.
Zhang, X., and J. E. Walsh (2006), Toward a seasonally ice-covered Arctic Ocean: Scenarios from the IPCC AR4 model simulations, *J. Clim.*, *19*, 1730–1747.

H. Eicken, Geophysical Institute, University of Alaska Fairbanks, 903 Koyukuk Drive, P.O. Box 757320, Fairbanks, AK 99775, USA.

K. F. Jones and D. K. Perovich, Cold Regions Research and Engineering Laboratory, U.S. Army Engineer Research and Development Center, 72 Lyme Road, Hanover, NH 03755, USA. (donald.k.perovich@erdc.usace.army.mil)

B. Light and K. Runciman, Polar Science Center, Applied Physics Laboratory, 1013 NE 40th Street, Seattle, WA 98105, USA.

S. V. Nghiem, Jet Propulsion Laboratory, California Institute of Technology, 4800 Oak Grove Drive, MS 300-235, Pasadena, CA 91109, USA.